General Disclaimer

One or more of the Following Statements may affect this Document

- This document has been reproduced from the best copy furnished by the organizational source. It is being released in the interest of making available as much information as possible.

- This document may contain data, which exceeds the sheet parameters. It was furnished in this condition by the organizational source and is the best copy available.

- This document may contain tone-on-tone or color graphs, charts and/or pictures, which have been reproduced in black and white.

- This document is paginated as submitted by the original source.

- Portions of this document are not fully legible due to the historical nature of some of the material. However, it is the best reproduction available from the original submission.

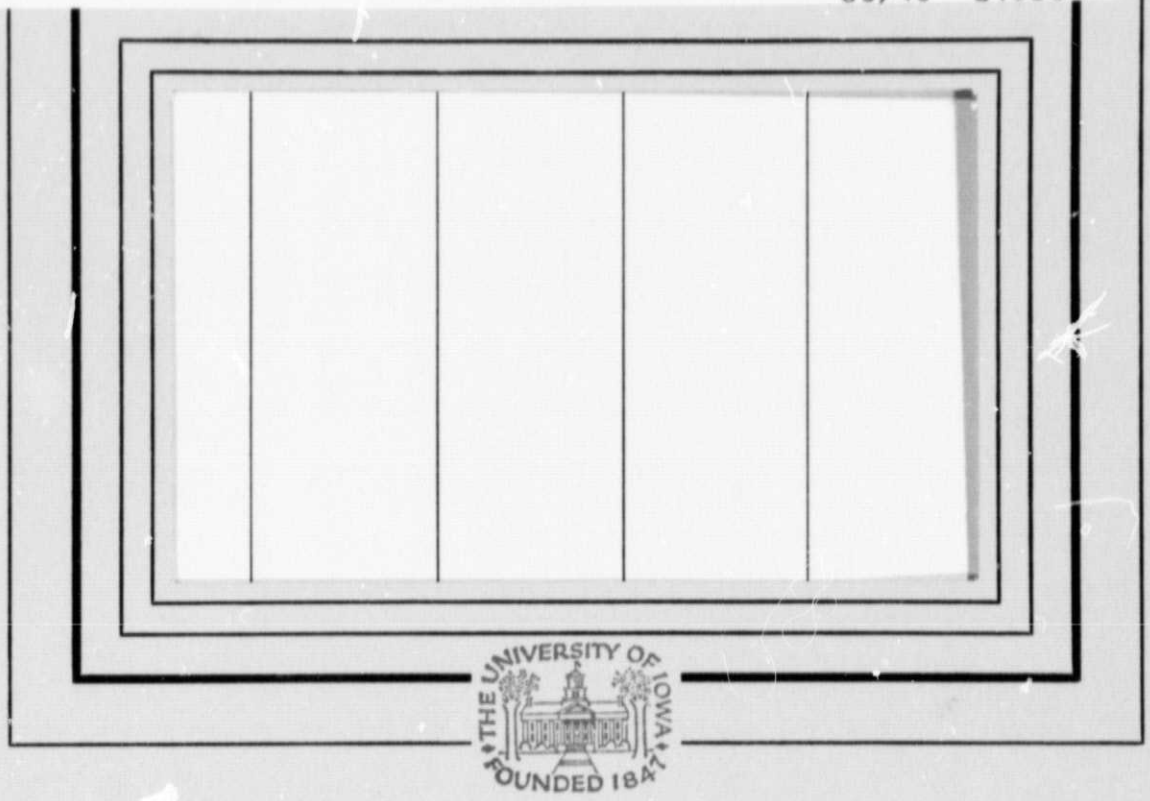

Research was supported in part by the Office of Naval Research
under contract N00014-68-A-0196-0009.

Department of Physics and Astronomy
THE UNIVERSITY OF IOWA
Iowa City, Iowa 52242

U. of Iowa 75-17

ELECTRON PRECIPITATION IN THE POST-MIDNIGHT SECTOR OF THE AURORAL ZONES*

by

L. A. Frank, N. A. Saflekos

and K. L. Ackerson

April 1975

Department of Physics and Astronomy
The University of Iowa
Iowa City, Iowa 52242

*Research supported in part by the National Aeronautics and Space Administration under contracts NAS5-10625, NAS1-8141, NAS1-2973 and grant NGL-16-001-002 and by the Office of Naval Research under contract N00014-68-A-0196-0009.

Abstract

Comprehensive measurements of the angular distributions and energy spectra of electron intensities within the energy range 50 eV $\leq$ E $\leq$ 15 keV with electrostatic analyzer arrays on board the low-altitude satellite Injun 5 are reported for the post-midnight sector of the auroral zones during the high-intensity events accompanying magnetic substorms. Precipitation features on closed terrestrial field lines well equatorward of the trapping boundary for energetic electrons with E > 45 keV are examined. No evidences of maxima in the differential energy spectra or of strongly field-aligned currents, $j_{\parallel} > j_{\perp}$, which are indicative of quasi-static electric fields aligned parallel to the geomagnetic field were found in our series of measurements within the above energy range. Precipitation of low-energy electron intensities fluctuated on time scales $\geq$ 2 seconds as viewed at the satellite position. This precipitation was characterized by isotropy for all pitch angles outside the atmospheric backscatter cone. Maximum precipitated energy fluxes were several ergs $(cm^2\text{-sec-sr})^{-1}$. This region of electron precipitation is associated with the diffuse aurora and with pulsating aurora in the post-midnight sector. Similar variations of the energetic electron intensities with E > 45 keV were observed in the regions of fluctuating energy fluxes of low energy electrons associated with auroral luminosity. In general the increases of energetic electron intensities were not coincident with those of the principal energy fluxes into the atmosphere, except when the average electron energy

for the energy fluxes was unusually high, i.e., in the 10-keV range. Precipitation of electron intensities within the energy ranges 50 eV to 15 keV and > 45 keV is consistent with strong pitch-angle diffusion of electron intensities near or at the magnetic equator by high-frequency wave turbulence, the effectiveness of which is modulated by perturbations attributable to micropulsations to yield the rapid fluctuations encountered over the post-midnight auroral zone.

I. Introduction

Extensive surveys of charged-particle precipitation into the auroral zones with earth satellites in nearly polar orbits at low altitudes have been reported previously, such as those with Injun 5 [Frank and Ackerson, 1972], OGO 4 [Hoffman and Burch, 1973], ISIS 1 [Heikkila and Winningham, 1971] and ESRO 1A [Hultqvist, 1974]. Several of the auroral precipitation zones have been specially concentrated upon with the desire of discerning the mechanisms for charged-particle entry into the magnetosphere, acceleration of these plasmas into the earth's upper atmosphere, and the sensitive responses of auroral features to fluctuations of solar wind parameters. Among these auroral domains are the low-altitude signature of the polar cusp, the inverted 'V' electron events and field-aligned currents, and the polar cap proper.

There is a striking contrast between the typical electron precipitation patterns observed in the local-evening and local-morning sectors of the auroral zone. In the local-evening sector are frequently found the intense, remarkable inverted 'V' events. These electron precipitation zones are easily identified in energy-versus-time

spectrograms of electron intensities by a clear increase in average electron energies to a maximum energy with a subsequent decrease of these electron energies as the observing satellite traverses these events [cf. Frank and Ackerson, 1971]. This phenomena is usually located near or poleward of the 'trapping boundary' for electrons with energies $\geq$ 50 keV. The position of this trapping boundary, or poleward termination of measurable energetic electron intensities, has been interpreted often as the approximate location for the boundary for closed field lines within the magnetosphere and those poleward field lines which are connected to interplanetary field lines within the magnetosheath. Equatorward of the inverted 'V' events and the trapping boundary, lesser intensities of electrons which can be identified as the low-altitude signature of the plasma sheet and its earthward extension as the ring current are persistently present. Whereas intense field-aligned electron intensities are found in inverted 'V' events, the electron angular distributions at these lower latitudes are typically isotropic outside of the atmospheric backscatter cone or with maximum directional intensities at pitch angles $\alpha = 90°$ [cf. Craven and Frank, 1975]. It is generally, but not unanimously thought that inverted-V events are attributable to

quasi-static electric fields directed parallel to the geomagnetic field [cf. Paulikas, 1971] and that the electron precipitation equatorward of these events is consistent with that expected for pitch-angle scattering of plasma-sheet electron intensities [cf. Kennel, 1969].

The overall character of electron intensities over the local-morning sector of the auroral zone differs substantially from that outlined above for local evening. The major electron precipitation zone is most often located well equatorward of the trapping boundary for energetic electrons, and intense inverted 'V' events are less frequently, by a factor of five or more, observed. Typically the region near and poleward of the trapping boundary is threaded with narrow, tens of kilometers, 'spikes' of electron intensities with average energies of only hundreds of eV or less [cf. Frank and Ackerson, 1972]. The energy input into the earth's upper atmosphere is dominated by the electron intensities at equatorward latitudes. These electrons have drifted into the local-morning sector of the magnetosphere from an injection and/or acceleration event positioned in the local-midnight, or magnetotail, sector [Hoffman, 1970; Frank and Ackerson, 1972]. Transport of these electrons is presumably effected by magnetic gradient and electric

field drifts. As these electrons drift from local midnight through the local-morning sector, their intensities lessen and average energies increase. Hoffman [1970] has associated the precipitation of these electron intensities into the upper atmosphere with the mantle aurora. Comprehensive measurements of the equatorial counterparts of these electron intensities at geosynchronous radial distances (6.6 R_E) have been reported by McIlwain [1972]. Considerably more information is needed concerning the pitch angle distributions of these electron intensities to delineate clearly the mechanism responsible for their precipitation into the auroral zones -- the principal topic of our present report.

Measurements of the angular distributions of electron intensities on closed field lines threading the local-morning sector were gained with the low-altitude satellite Injun 5 which was equipped with electrostatic analyzers, or LEPEDEA's, for detailed plasma measurements. These measurements are reported for two periods: (1) the first few months after launch when the satellite was spinning about a known axis and allowed sampling of a large range of pitch angles α and (2) during magnetic alignment of the satellite, which provided good temporal resolution of intensities at $\alpha = 0°$ (into the atmosphere) and $\alpha = 90°$

(mirroring). These angular distributions are examined for evidences of strong pitch-angle scattering and field-aligned currents within the electron energy range extending from 50 eV to 15 keV.

II. Observations

The measurements of low-energy electron intensities reported herein were gained with electrostatic analyzers on board the low-altitude, polar-orbiting satellite Injun 5. The perigee and apogee altitudes were 677 and 2528 km, respectively, and the orbital inclination was 81° on the launch date August 8, 1968. The satellite spin rate decreased by early December of the same year to sufficiently small values to allow magnetic alignment of the satellite with the local terrestrial field by means of two parallel Alnico-V bar magnets. Effective magnetic alignment is known to have continued from this time until cessation of our ground station activities on May 30, 1970. Observations of low-energy electron intensities with two electrostatic analyzers, or LEPEDEA's, and their companion Geiger-Mueller tubes are reported here for the periods before and after magnetic alignment. The Geiger-Mueller tubes respond primarily to directional intensities of electrons with $\dot{E} > 45$ keV at auroral latitudes. Each LEPEDEA instrument is capable of measuring the directional, differential intensities of electrons and positive ions over the energy range 5 eV to 50 keV. For the instrument

operational mode employed here this energy range was restricted to the range 50 eV to 15 keV. The reader is referred to previously published literature for further information concerning these electrostatic analyzers [Frank, 1967; Frank et al., 1966]. During the period of alignment commencing in December 1968 the axes of the fields-of-view of one of the electrostatic analyzers (LEPEDEA 'A') were directed anti-parallel to the local magnetic field vector, or upward over the Northern hemisphere, and those of the second analyzer (LEPEDEA 'B') were directed orthogonal to the magnetic field vector. The axes of the fields-of-view of two collimated, thin-windowed Geiger-Mueller tubes were positioned parallel to those of the two LEPEDEA's, respectively. Hence during this period of magnetic alignment angular distributions of low-energy electron and proton intensities, as well as of electron intensities at $E > 45$ keV, at the two pitch angles $\alpha = 0°$ and $90°$ are available.

During October 1968, prior to satellite magnetic alignment, the orientation of the spin axis relative to the satellite coordinates was such that the axes of the fields-of-view of one of the LEPEDEA's, LEPEDEA 'B', were directed nearly parallel to the spin vector and those of the second analyzer, LEPEDEA 'A', were nearly perpendicular

to the spin vector. This occasion allowed LEPEDEA 'A' to sample a broad range of pitch angles in the local-morning sector of the auroral zone. The spin periods for the two such auroral passes examined in detail here, Revolutions 797 and 870, were 52 and 60 seconds, respectively. Each LEPEDEA was operated in a scan mode which provided a 117-sample energy spectrum of electron intensities, 50 eV $\leq$ E $\leq$ 15 keV, in 910 msec once each 2-second interval. In other words, during a spin period of 60 seconds, 30 electron spectra were telemetered from each LEPEDEA. The instantaneous pitch angles corresponding to the directions of the fields-of-view of these electrostatic analyzers were determined with the telemetered responses of the satellite magnetic aspect sensors, solar aspect sensors and solar panel thermistors. This aspect information was merged with the corresponding LEPEDEA responses to gain the pitch angle distributions of electron intensities, as functions of electron energy, reported here.

These observations for the period prior to magnetic alignment were restricted in several ways, although these restrictions do not lessen their importance. First a relatively stable spin axis was required in order to

accurately calculate the pitch angles sampled by the instruments. This necessity eliminated a portion of the possible observational period prior to magnetic alignment. Next a favorable orientation of the spin axis relative to the magnetic field vector over the Northern auroral zones was desired for sampling an extensive range of pitch angles. The usual requirement of quality telemetry eliminated further traverses over the auroral zones. Since the satellite was also often employed at its lower telemetry rate for survey purposes during the initial stages of ground station operations, this factor also took a substantial toll since high bit-rate telemetry is required for meaningful sampling of the energy spectra as functions of pitch angle. And finally, observations associated with geomagnetically active periods provide the best opportunities for examination of the character of electron precipitation, since the electron intensities are substantially greater and the precipitation zone is significantly broader in latitude relative to those encountered during periods of relative magnetic quiescence. Correspondingly our present measurements are associated with periods of magnetic substorm activity.

An example of observations of the angular distributions of electron intensities over the local-morning sector

of the auroral zone while the satellite is spinning is summarized in the color-coded energy-time spectrogram of Figure 1. Responses of LEPEDEA 'A' to directional electron intensities are color coded according to the scale at the right-hand side of the spectrogram. Low responses are coded blue, high responses are red. The labels on the scale are the $\log_{10}$ of the instrument responses in counts $(sec)^{-1}$. These color-coded detector responses are plotted as functions of electron energy (ordinate) and Universal Time (abscissa) to form the energy-time (E-t) spectrogram shown in Figure 1 (see also Frank and Ackerson [1971]). Invariant latitude (Λ), local scalar magnetic field (B) and magnetic local time (MLT) are also given along the abscissa. The periodic, vertical blue lines, e.g., at 0834:50 U.T., are small responses due to solar ultraviolet as LEPEDEA 'A' scans the sun. For this traversal of the auroral zones the satellite is moving equatorward. Intense electron intensities were encountered over the period 0828:10 to 0830:30 U.T. and are located equatorward of the trapping boundary as determined by perusal of the G.M. tube responses to energetic electron intensities.

The spin-modulation of electron intensities for the auroral zone traversal of Figure 1 is readily apparent. In order to examine several of the salient features of

the pitch-angle distributions of these electron intensities, we have plotted the directional, differential intensities at two energies, 100 eV and 1 keV, as functions of U.T. in Figure 2. Measurements with both LEPEDEA's 'A' and 'B' have been included, as well as the instantaneous pitch angles for each of these analyzers. First note that the pitch angles sampled by LEPEDEA 'B' range within 10° of 120°, corresponding to mirror points at sufficiently high altitudes to preclude major energy loss and scattering attributable to the atmosphere. The overall profiles of electron intensities at 100 eV and 1 keV within this pitch angle range (open circles) display no severe variations indicative of large temporal or spatial variations in intensities. The measurements with LEPEDEA 'B' at relatively constant pitch angles provide useful reference measurements for the pitch-angle scans with LEPEDEA 'A'. The range of pitch angles sampled by LEPEDEA 'A' during this series of observations was approximately 20° to 160°. The LEPEDEA fields-of-view are approximately rectangular, 8° x 20°. For LEPEDEA 'A' the 8° dimension was nearly parallel to the satellite spin axis. Comparing the intensity measurements of the two electrostatic analyzers as summarized in Figure 2, we find isotropy of intensities at all pitch angles outside

of the effective atmospheric backscatter cone at $\alpha \geq 140°$ and well-defined minima of intensities, by factors of 5 to 10, within the backscatter cone. There is no evidence of strong field-aligned currents, i.e., $j(\alpha = 0° \text{ or } 180°) > j(\alpha = 90°)$, in this series of measurements. However, the isotopy of intensities over the upper hemisphere of pitch angles centered at $\alpha = 0°$ and the minimum of intensities within the backscatter cone are indicative of a net flux of electrons into the upper atmosphere -- an upward flowing Birkeland current. The angular distributions are immediately suggestive of strong pitch-angle diffusion occurring at some location along these magnetic field lines.

The differential energy spectra of electron intensities for a segment of the observations of Figures 1 and 2 are given in Figure 3. Smoothed curves through each of the 117-sample electron spectra are shown in order to enhance the visual clarity. The period covered by Figure 3 is 0829:03 to 0829:49 U.T. (cf. Figure 2). The angular distributions are notably isotropic for all pitch angles outside of the atmospheric backscatter cone for all energies within the range 50 eV to 15 keV. Measurements within the backscatter cone are to be found at the bottom of the second column and top of the third

column of Figure 3. Intensities of electrons with energies $\geq$ 200 eV are typical of those found in the corresponding sector of the equatorial magnetosphere [cf. Frank, 1971; DeForest and McIlwain, 1971]. No substantial secondary maxima of differential intensities, which would be indicative of acceleration by parallel quasi-static electric fields, is evident in this series of observations.

A second, similar series of measurements are summarized in the E-t diagram for Revolution 797 of Figure 4. Again the satellite is moving equatorward over the local-morning sector of the auroral zone. Major electron intensities were encountered over the time interval 0826:55 to 0830:30 U.T. Differential electron intensities at 100 eV and 1 keV are shown in Figure 5. Again the electron intensities outside the effective backscatter cone are isotropic within factors of 2 or 3 and intensities inside the backscatter cone are lesser by factors of 5 to 10. Temporal and spatial variations in intensities at pitch angles outside of the backscatter cone appear limited to factors of 2 to 3 with the exception of the event centered at about 0827:20 U.T., which is an increase over the smoothed-profile intensities by a factor of 20 at electron energies of 1 keV. It is not

possible to identify this event uniquely as a spatial or temporal feature. Electron spectra for the segment of observations spanning 0827:46 to 0828:32 U.T. are shown in Figure 6. As for the previous series of measurements, there is no evidence of strong field-aligned currents, $j_{\parallel} > j_{\perp}$, or of secondary spectral maxima which are an inviting signature of the presence of an electric field directed parallel to the geomagnetic field.

The foregoing measurements of electron intensities along closed field lines well equatorward of the trapping boundary in the local-morning sector of the auroral zones set the stage for utilizing the greater temporal and spatial resolution available at two pitch angles during satellite magnetic alignment. Specifically we have shown that the electron intensities are isotropic, within factors of 2 or 3, at pitch angles outside of the backscatter cone for the energy range 50 eV to 15 keV. Further, there was no evidence of secondary maxima in the electron energy spectra, which are suggestive of acceleration by parallel electric fields. These electron intensities are identified with those of electrons of the equatorial plasma sheet, which are drifting through the morning sector of the magnetosphere. More information

concerning these electron intensities may be gained by examining the following observations at the two pitch angles $\alpha = 0°$ (precipitating) and 90° (mirroring) in the post-midnight sector during satellite magnetic alignment.

Such an example of measurements of precipitated electron intensities is offered in the spectrogram of Figure 7. As the satellite moves equatorward from the polar cap region it first encountered a relatively weak inverted 'V' event centered at 0645:00 U.T., then the trapping boundary at about 0645:30 U.T. and hence into the electron intensities associated with the equatorial plasma sheet -- this latter event bears the main thrust of our present discussion. Careful examination of the character of the spectrogram during the encounter with these plasma sheet intensities at about 0645:30 to 0647:30 U.T. reveals a pulsation of intensities with periods ranging 2 to 5 seconds (the temporal resolution is 2 seconds per telemetered spectrum). We will return to these fascinating pulsations after examination of the energetic electron intensities for similar behavior.

Simultaneous measurements of electron intensities with $E > 45$ keV at pitch angles $\alpha = 0°$ and 90° are shown in Figure 8. The upper envelopes of the thickly inked

profiles are mirroring electron intensities at $\alpha = 90°$; the bottom envelopes are precipitated electron intensities at $\alpha = 0°$. From top to bottom panels, the temporal resolution of the measurements increases. The temporal resolution for the observations of the bottom panel is 30 msec. Segments of the measurements for the various panels are designated by the dotted lines. The entire set of measurements in the bottom panel corresponds to the time period designated by the width of the small solid dot in the top panel. The lower temporal resolutions of the top and middle panels were obtained by straightforward averaging of 30-msec intensity samples. The top panel shows that energetic electron precipitation accompanies the low-energy electron precipitation from the plasma sheet at about 0645:30 to 0647:00 U.T. (cf. Figure 7). The middle panel establishes the existence of variations of precipitated electron intensities on temporal scales of seconds as seen at the satellite position. And the lower panel yields evidence of such variations as fast as 30 to 60 msec, or about 150 to 300 m of satellite orbital motion. Since the gyroradii for mirroring electrons with $E \simeq 50$ keV are only several tens of meters at the satellite position, it is not possible to discern whether the severe fluctuations of electron

intensities displayed in either Figure 7 or 8 are spatial or temporal variations with these observations only. However, it is possible to conclude that the precipitation mechanism scatters electrons into the atmospheric loss cone without any substantial variations in intensities of mirroring electrons (see Figure 8). Furthermore this pitch angle scattering is capable of increasing precipitated electron intensities to isotropy over the upper hemisphere of pitch angles often, but not always. No evidence of strongly field-aligned intensities of energetic electrons, $j(\alpha = 0°) > j(\alpha = 90°)$, is evident in this and the following series of measurements. The smoothly varying profiles of electron intensities at $\alpha = 90°$ suggest that the dramatic variations associated with the precipitated intensities can be observed only within a few degrees or less of the magnetic vector at the equator. In brief summary large variations of electron intensities precipitated into the atmosphere by pitch angle scattering are observed at low altitudes on closed field lines populated with electrons of plasma-sheet origins -- these variations taken alone could be interpreted as temporal variations of the entire precipitation zone, isolated spatial structures within this zone or a combination of both.

It is of interest to examine the relationship between the precipitation of energetic electron intensities of Figure 8, which will produce auroral X-ray emission, with that of the lower-energy electron intensities as shown in Figure 7, which are associated with auroral luminosity. Precipitated and mirroring electron intensities with $E > 45$ keV are summarized in the upper two panels of Figure 9. These electron intensities have been averaged over two-second intervals corresponding to the temporal resolution for measuring the mirroring and precipitated energy fluxes of electrons within the energy range 50 eV to 15 keV. These energy fluxes are given in the lower two panels of Figure 9. The fluctuations of precipitating energy fluxes are substantially greater than those for mirroring electron intensities. Maximum energy fluxes are small, typically only several ergs $(cm^2\text{-sec-sr})^{-1}$, compared to maximum energy fluxes ranging to several hundreds of ergs $(cm^2\text{-sec-sr})^{-1}$ for an inverted 'V' event. Further, maxima of energy fluxes at $\alpha = 0°$ and $90°$ are not always coincident, even though the samples of energy spectra are gained simultaneously. In order to determine whether or not electron precipitation occurs simultaneously for electrons with $E > 45$ keV and $50 \text{ eV} \leq E \leq 15$ keV. We have plotted the ratios of electron intensities and energy fluxes, respectively,

in Figure 10. As with the electron intensities with E > 45 keV, energy fluxes of lower energy electrons are not found to be field-aligned in this precipitation zone. Precipitation events are associated with near-isotropy over the upper hemisphere of pitch angles as shown in the lower panel of Figure 10, within the accuracy of absolute determination of electron intensities with the LEPEDEA's of ±25%. The times for precipitation events, or isotropies, for the low-energy electron fluxes are identified via solid circles in the upper panel which displays the corresponding ratios for energetic electron intensities. This comparison yields the conclusion that enhanced pitch-angle scattering of energetic electrons is not generally coincident with that for low-energy electron intensities at the satellite position -- hence X-ray and optical aurora as observed from ground-based stations would not be necessarily spatially coincident or in phase.

If the mechanism for strong pitch-angle scattering is one and the same for both the low-energy and energetic electron intensities as the above observations suggest, but is located at the equator, then the dispersion associated with propagation times for motion from equator to satellite position would preclude the possibility of simultaneity of precipitation for these two energy

regimes. For a 500-eV electron the flight time from equator to atmosphere at these geomagnetic latitudes is roughly 10 sec. The typical average electron energy for the observations of Figures 7 and 10 is 500 eV. Correspondingly, if we expect to encounter an electron precipitation event which would yield coincident X-ray and visual aurora then the average electron energies for the principal energy fluxes must be substantially greater than the foregoing example -- in the range of 10 keV. A traversal of such a precipitation event is shown in the spectrogram for Revolution 3619 in Figure 11. As for previous passes the satellite is moving equatorward. The precipitation zone of special interest here was encountered at 0744:40 to 0745:30 U.T. and is characterized by notably high fluxes of electrons in the 10-keV energy range. As a side note of relatively minor interest here, there are four identifiable, but diminutive inverted 'V' events centered at 0740:45, 0741:10, 0741:58 and 0742:50 U.T., in the poleward precipitation zones of Figure 11. Returning to the equatorward precipitation zone which is located without question on closed field lines equatorward of the trapping boundary, we have summarized measurements of electron energy fluxes for the energy range $50 \leq E \leq 15$ keV and

electron intensities with E > 45 keV in the top and bottom panels, respectively, of Figure 12. Observations at both pitch angles $\alpha = 0°$ and $90°$ are shown. Precipitation of energetic electrons occurs within the regions of greatest energy fluxes of lower energy electrons but does not span the latter regions in their entirety. Peak energy fluxes precipitating into the atmosphere are again in the range of several ergs $(cm^2\text{-sec-sr})^{-1}$ and are associated with pitch angle distributions which are driven to isotropy over the upper hemisphere of pitch angles. Precipitation features for these two electron energy ranges do not appear coincident for the event centered at about 0743:15 U.T. -- however, the energy fluxes are dominated by electrons in the keV range of energies. These average electron energies are sufficiently great for the event centered at about 0745:00 U.T. to yield such simultaneity of precipitation. This correlation of intensities as measured at the satellite position is further demonstrated by the comparison of electron intensities at 10.4 keV, dJ/dE, and 45 keV, J(>E), offered in Figure 13 (specifically, the period 0744:40 to 0745:30 U.T.). Emissions of X-rays and of optical emissions for this auroral precipitation event would indeed be coincident.

III. Discussion

Our specific intent in the preceding presentation of observations was to examine the character of the energy spectra and angular distributions of low-energy electron intensities at low altitudes in the post-midnight sector of the auroral zones, which were associated with substorm activity. This analysis was directed toward yielding further information concerning the mechanism responsible for electron precipitation along magnetic field lines which are closed within the terrestrial magnetosphere and are located substantially equatorward of the trapping boundary for energetic electrons. The electron energy ranges were $50\ \text{eV} \leq E \leq 15\ \text{keV}$ and $E > 45\ \text{keV}$. Our principal results are:

- no evidence of secondary maxima in the electron energy spectra or strongly field-aligned intensities, $j(\alpha = 0°) > j(\alpha = 90°)$, which are indicative of quasi-static electric fields directed parallel to the geomagnetic field,
- isotropic electron intensities within factors of 2 or 3 for the energy range $50\ \text{eV} \leq E \leq 15\ \text{keV}$ at all pitch angles outside the atmospheric backscatter cone, with intensities in the backscatter cone lesser by factors of 5 to 10,

- Birkeland currents associated with this precipitation are of the order of 1 $\mu a(m)^2$ directed out of the ionosphere,
- fluctuations of the energy fluxes of low energy electrons precipitated into the earth's atmosphere as observed at the satellite position were characterized by increases by factors typically 2 or 3 to isotropy outside the backscatter cone, which were accompanied by relatively minor increases of mirroring energy fluxes.
- maximum precipitated energy fluxes for the energy range 50 eV $\leq$ E $\leq$ 15 keV were several ergs $(cm^2\text{-sec-sr})^{-1}$ and time scales for fluctuations of these fluxes were about 2 to 10 sec,
- precipitated energy fluxes decreased to typical values of tenths of an erg $(cm^2\text{-sec-sr})^{-1}$ between energy flux maxima, indicating that a loss mechanism was continu lly present during our encounters with this portion of the auroral zone,
- dramatic variability of precipitating energetic electron intensities with E > 45 keV generally accompanied the above fluctuations of low-energy electron intensities, with the occasional exception when the latter were encountered without large variability of electron (E > 45 keV) intensities,

- time scales for major fluctuations of energetic electron intensities were similar to those for the energy fluxes of electrons in the range 50 eV $\leq$ E $\leq$ 50 keV, 2 to 10 seconds,
- increases of precipitated energetic electron intensities displayed the same overall character as those of low-energy electron intensities with the exception of peak-to-valley ratios which often increased to factors $\geq$ 10,
- increases of precipitated energetic electron intensities were not simultaneous with those for energy fluxes except when the average electron energies for these energy fluxes were high, in the range of 10 keV, (if the mechanisms responsible for this precipitation are indeed one and the same, and we have found no need to assume otherwise from our measurements, this feature places the position for the strong pitch-angle scattering at great distances from the satellite, tens of thousands of km and probably near the equator), and
- it is not possible to identify these rapid fluctuations of electron intensities as seen at the satellite position as spatial or temporal variations (or a combination of both) with these observations alone.

Further information concerning the possible identification of these fluctuations of electron intensities as spatial or temporal variations can be obtained from ground-based optical measurements and balloon-borne X-ray detectors. Our observations are almost certainly gained in the segment of the auroral zone characterized by pulsating aurora: quasi-periodic intensity variations in the range 1 to 10 or more sec, low intensities, eastward drift, maximum occurrence in the few hours following local midnight, appearance during magnetic substorms, spatial dimensions of the orders 0.2 to 50 km or more, and positions favoring the equatorward boundary of auroral luminosity [cf. Heppner, 1954; Cresswell and Davis, 1966]. These criteria are all satisfied by our measurements. Hence we conclude that most likely the fluctuations reported here are the signatures of both temporal and spatial variations and are to be associated with the phenomena of pulsating aurora. A great host of literature concerning auroral X-ray pulsations is available in the literature (cf. reviews by Brown [1966] and Anderson [1968]). Of immediate interest to the present discussion are the quasi-periodic pulsations of X-rays associated with the precipitation of electrons with $E \geq 45$ keV, which are in the range of 5 to 15 sec for

the local morning sector of the auroral zones during substorms [Parks et al., 1968]. The spatial dimensions at the satellite altitudes are typically hundreds of km [Barcus and Rosenberg, 1965, Parks et al., 1968]. Hence the presently reported fluctuations of precipitating energetic electron intensities are probably the signature of spatial and temporal variations. However, returning to a specific observation as an example, that for the time interval 0744:30 to 0745:30 U.T. of Figure 13, we would assume that this 'patch' of precipitation with spatial dimensions of about 300 km (from satellite motion) is pulsating with a quasi-period of ~10 sec (approximately 6 unequal maxima of intensities in 60 seconds) in the spirit of the present interpretation.

The most promising mechanism which would account for our observations has been presented by Coroniti and Kennel [1970]. During magnetic substorms electron intensities are presumed to be enhanced above the critical intensities for whistler instability, or other high-frequency wave turbulence, near the magnetic equator. This situation will disturb the pitch-angle equilibrium of the electrons with the wave turbulence, resulting in loss of electrons via the atmospheric loss cone. Sustained precipitation implies a strong source for electron intensities.

Pulsations in the intensities of electrons precipitating into the atmosphere can be effected by the presence of micropulsations with periods of seconds to several hundred of seconds. The effects of the micropulsations would be expected to be weak if the electron intensities are not near critical intensities, not only because of the relatively small amplitudes of the micropulsations but also since the second and third adiabatic invariants for the electrons would be conserved. However, at the critical intensities for these electrons small perturbations due to the presence of micropulsations should induce strong modulation of precipitating electron intensities via compression and decompression of the electron distribution function and variations in the propagation of the wave turbulence. Remarkably enough, all aspects of electron precipitation in the post-midnight sector of the aurora zones associated with substorm activity as reported here are in substantial qualitative agreement with the above postulated mechanism.

Further useful approaches for studies of this electron precipitation phenomenon of strong, variable pitch-angle diffusion have employed rocket flights to gain access to individual magnetic flux tubes of electron intensities for more extended periods of time [cf. Evans,

1971] and coordinated rocket-borne observations of precipitating electron intensities and ground-based measurements of pulsating patches of luminosity [cf. Whalen et al., 1971 and Rosenberg et al., 1967]. Recent global imaging of auroral luminosity from the perspective of earth satellites provides a special tool for identifying the general character of the auroral zone of interest -- in this case, the 'diffuse' aurora [Lui and Anger, 1973]. The promising possibility of measuring electron intensities within the atmospheric loss cones at the magnetic equator, and hence in situ observations of the strong pitch-angle diffusion, is offered by the plasma instrumentation on the recently launched, geosynchronous satellite ATS 6 [McIlwain, 1975]. For this major electron precipitation zone in the post-midnight sector of the auroral zone it would appear that expectations of a comprehensive understanding of the participating mechanisms in the near future are not unwarranted.

Acknowledgments

This research was supported in part by the National Aeronautics and Space Administration under contracts NAS5-10625, NAS1-8141, NAS1-2973 and grant NGL-16-001-002 and by the Office of Naval Research under contract N00014-68-A-0196-0009.

References

Anderson, K. A., Wave-Energetic Particle Associations in the Magnetosphere, Earth's Particles and Fields, ed. by B. M. McCormac, p. 429, Reinhold Book Corp., New York, 1968.

Barcus, J. R. and T. J. Rosenberg, Observations on the Spatial Structure of Pulsating Electron Precipitation Accompanying Low-Frequency Hydromagnetic Disturbances in the Auroral Zone, J. Geophys. Res., 70, 1707, 1965.

Brown, R. R., Electron Precipitation in the Auroral Zone, Space Sci. Rev., 5, 311, 1966.

Coroniti, F. V. and C. F. Kennel, Auroral Micropulsation Instability, J. Geophys. Res., 75, 1863, 1970.

Craven, J. D. and L. A. Frank, Observations of Angular Distributions of Low-Energy Electron Intensities Over the Auroral Zones with Ariel 4, to be published in Proceedings of The Royal Society, 1975.

Cresswell, G. R. and T. N. Davis, Observations on Pulsating Auroras, J. Geophys. Res., 71, 3155, 1966.

DeForest, S. E. and C. E. McIlwain, Plasma Clouds in the Magnetosphere, J. Geophys. Res., 76, 3587, 1971.

Evans, D. S., Direct Observation of Temporal and Spatial Structure in Auroral Electrons, The Radiating Atmosphere, ed. by B. M. McCormac, p. 267, D. Reidel Publishing Company, Dordrecht; Holland, 1971.

Frank, L. A. Initial Observations of Low-Energy Electrons in the Earth's Magnetosphere with Ogo 3, J. Geophys. Res., 72, 185, 1967.

Frank, L. A., Relationship of the Plasma Sheet, Ring Current, Trapping Boundary, and Plasmapause near the Magnetic Equator and Local Midnight, J. Geophys. Res., 76, 2265, 1971.

Frank, L. A. and K. L. Ackerson, Observations of Charged Particle Precipitation into the Auroral Zone, J. Geophys. Res., 76, 3612, 1971.

Frank, L. A. and K. L. Ackerson, Local-Time Survey of Plasma at Low Altitudes over the Auroral Zones, J. Geophys. Res., 77, 4116, 1972.

Frank, L. A., W. W. Stanley, R. H. Gabel, D. C. Enemark, R. F. Randall, and N. K. Henderson, Technical Description of LEPEDEA Instrumentation (Injun 5), Univ. Iowa Res. Rep. 66-31, Iowa City, 196 .

Gurnett, D. A. and L. A. Frank, Continuum Radiation From Energetic Electrons in the Outer Radiation Zone, J. Geophys. Res., (to be published), 1975.

Heikkila, W. J. and J. D. Winningham, Penetration of Magnetosheath Plasma to Low Altitudes Through the Dayside Magnetospheric Cusps, J. Geophys. Res., 76, 883, 1971.

Heppner, J. P., A Study of the Relationships Between the Aurora Borealis and the Geomagnetic Disturbances Caused by Electric Currents in the Ionosphere, (thesis), California Institute of Technology, 1954.

Hoffman, R. A., Auroral Electron Drift and Precipitation: Cause of the Mantle Aurora, NASA-GSFC X-646-70-205, June 1970.

Hoffman, R. A. and J. L. Burch, Electron Precipitation Patterns and Substorm Morphology, J. Geophys. Res., 78, 2867, 1973.

Hultqvist, B., Evidence from Particle Precipitation of Two-Way-Convection in Auroral Latitudes, J. Geophys., 40, 713, 1974.

Kamide, Y. and C. E. McIlwain, The Onset Time of Magnetospheric Substorms Determined From Ground and Synchronous Satellite Records, J. Geophys. Res., 79, 4787, 1974.

Kennel, C. F., Consequences of a Magnetospheric Plasma, Rev. Geophys. Space Phys., 7, 379, 1969.

Lui, A. T. Y. and C. D. Anger, A Uniform Belt of Diffuse Auroral Emission Seen by the ISIS-2 Scanning Photometer, Planet. Space Sci., 21, 799, 1973.

McIlwain, C. E., Plasma Convections in the Vicinity of the Geosynchronous Orbit, Earth's Magnetospheric Processes, ed. by B. M. McCormac, p. 268, Reidel Publishing Co., Dordrecht, Holland, 1972.

McIlwain, C. E., Data From ATS 6 and Their Interpretation, Proceedings of the Nobel Symposium on the Physics of the Hot Plasma in the Magnetosphere, (to be published), 1975.

Parks, G. K., F. V. Coroniti, R. L. McPherron, and K. A. Anderson, Studies of the Magnetospheric Substorm, 1, Characteristics of Modulated Electron Precipitation Occurring During Auroral Substorms, J. Geophys. Res., 73, 1685, 1968.

Paulikas, G. A., The Patterns and Sources of High-Latitude Particle Precipitation, Rev. Geophys. Space Phys., 9, 659, 1971.

Rosenberg, T. J., J. Bjordal, and G. J. Kvifte, On the Coherence of X-Ray and Optical Pulsations in Auroras, J. Geophys. Res., 72, 3504, 1967.

Whalen, B. A., J. R. Miller, and I. B. McDiarmid, Energetic Particle Measurements in a Pulsating Aurora, J. Geophys. Res., 76, 978, 1971.

World Data Center A, Auroral Electrojet Magnetic Activity Indices AE (11) For 1968 and 1969, Reports UAG-29 (1968) and UAG-39 (1969), NOAA, Boulder, Colorado, (1968) 1973; (1969) 1974.

Figure Captions

Figure 1. Color-coded E-t spectrogram of electron intensities for a crossing of the local-morning sector of the auroral zones on October 19, 1968. These observations with LEPEDEA 'A' were taken during the period of satellite spin, or 'cartwheel' mode, which preceded magnetic alignment of the satellite. The corresponding AE index was 99 γ(gammas) [World Data Center A, 1973] and a small magnetic bay ($\sim$ 100 γ) is discernible in the Great Whale magnetograms. The onset of a substantial substorm is evident in the College magnetograms just prior to 0900 U.T. However, the electron intensities at lower latitudes may have been injected onto these field lines during a substorm hours before this particular series of measurements [cf. Kamide and McIlwain, 1974; Gurnett and Frank, 1975].

Figure 2. Directional, differential electron intensities at 100 eV and 1 keV as functions of Universal Time for the period of major precipitation of Figure 1. Measurements with both electrostatic analyzer arrays, LEPEDEA's 'A' and 'B', are displayed here. Corresponding pitch angles for these measurements are given in the bottom panel.

Figure 3. Directional, differential spectra of electron intensities for the segment of observations spanning 0829:03 to 0829:49 U.T. of Figure 1. Simultaneous measurements with LEPEDEA's 'A' and 'B' are shown.

Figure 4. Continuation of Figure 1 for October 13, 1968. The AE index was 462 γ.

Figure 5. Continuation of Figure 2 for the series of measurements of October 13, 1968.

Figure 6. Continuation of Figure 3 for the series of measurements of October 13, 1968 (0827:46 to 0828:32 U.T.).

Figure 7. Continuation of Figure 1 for June 5, 1969 after the satellite had achieved

magnetic alignment. Hence this E-t spectrogram solely displays electron intensities at pitch angle $\alpha = 0°$ (precipitating into the atmosphere). The AE indices ranged from 70 γ to 378 γ during the first eight hours of June 5 [World Data Center A, 1974].

Figure 8. Simultaneous measurements of the directional intensities of electrons with E > 45 keV at pitch angles $\alpha = 0°$ and 90° corresponding to the series of observations of Figure 7. Increasing temporal resolutions are displayed from top to bottom panels.

Figure 9. Comparison of electron intensities with E > 45 keV and energy fluxes for electron intensities with 50 eV ≤ E ≤ 15 keV at $\alpha = 0°$ (precipitating) and $\alpha = 90°$ (mirroring) corresponding to the low-latitude segment of the E-t spectrogram of Figure 7.

Figure 10. The ratios of the precipitating intensities and energy fluxes to those for mirroring electrons corresponding to the observations of Figure 9.

Figure 11. Continuation of Figure 7 for June 2, 1969. The AE index was 354 γ. Magnetic substorm onset (Great Whale) was approximately four hours prior to these measurements.

Figure 12. Simultaneous observations of energetic electron intensities with E > 45 keV (lower panel) and electron energy fluxes for 50 eV $\leq$ E $\leq$ 15 keV (upper panel) at $\alpha = 0°$ and 90° for the low-latitude segment of the E-t spectrogram of Figure 11.

Figure 13. Comparison of the intensities of electrons with E > 45 keV and differential electron intensities at 10.4 keV for the major precipitation event centered at 0745 U.T. of Figure 12.

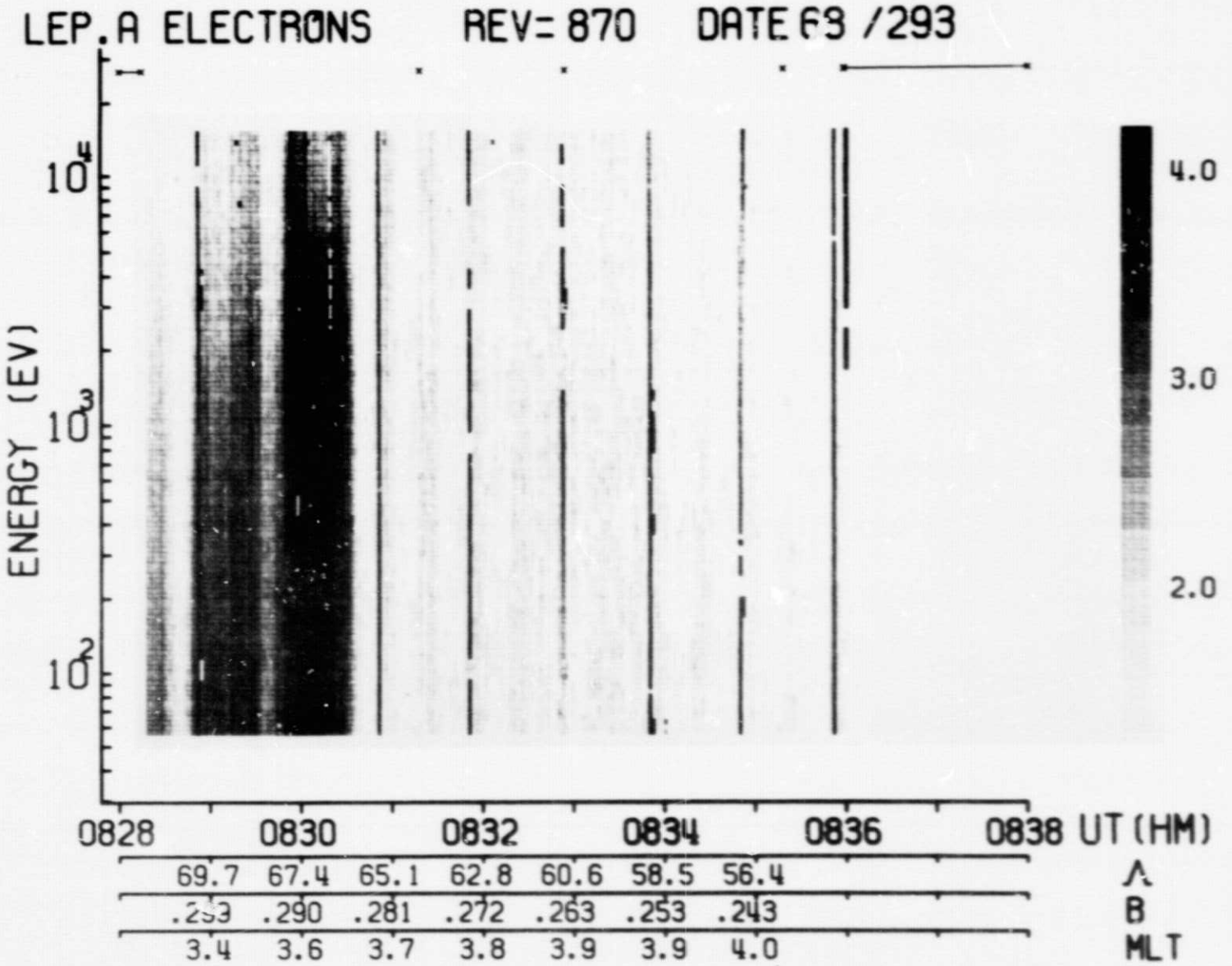

Figure 1.

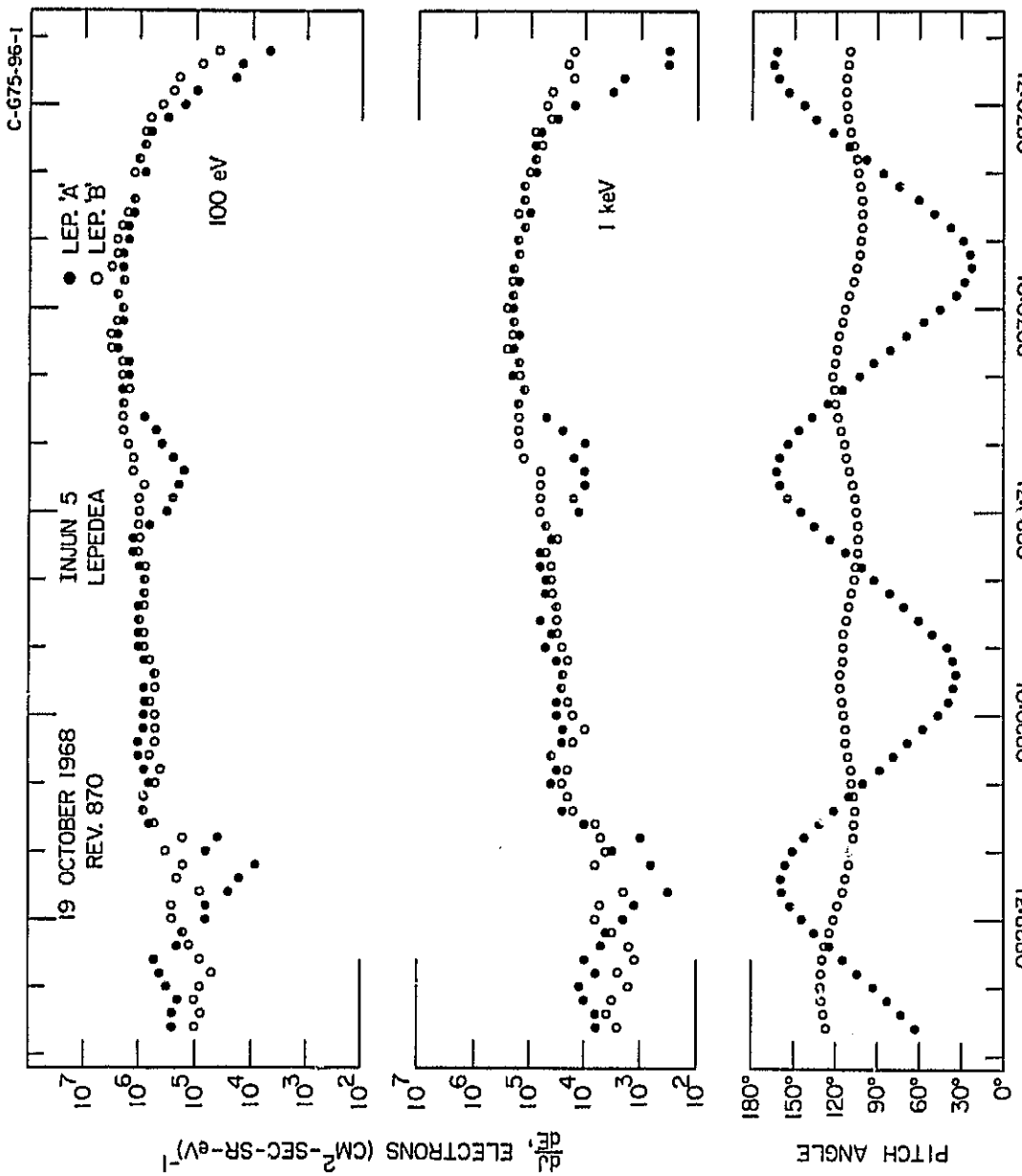

Figure 2.

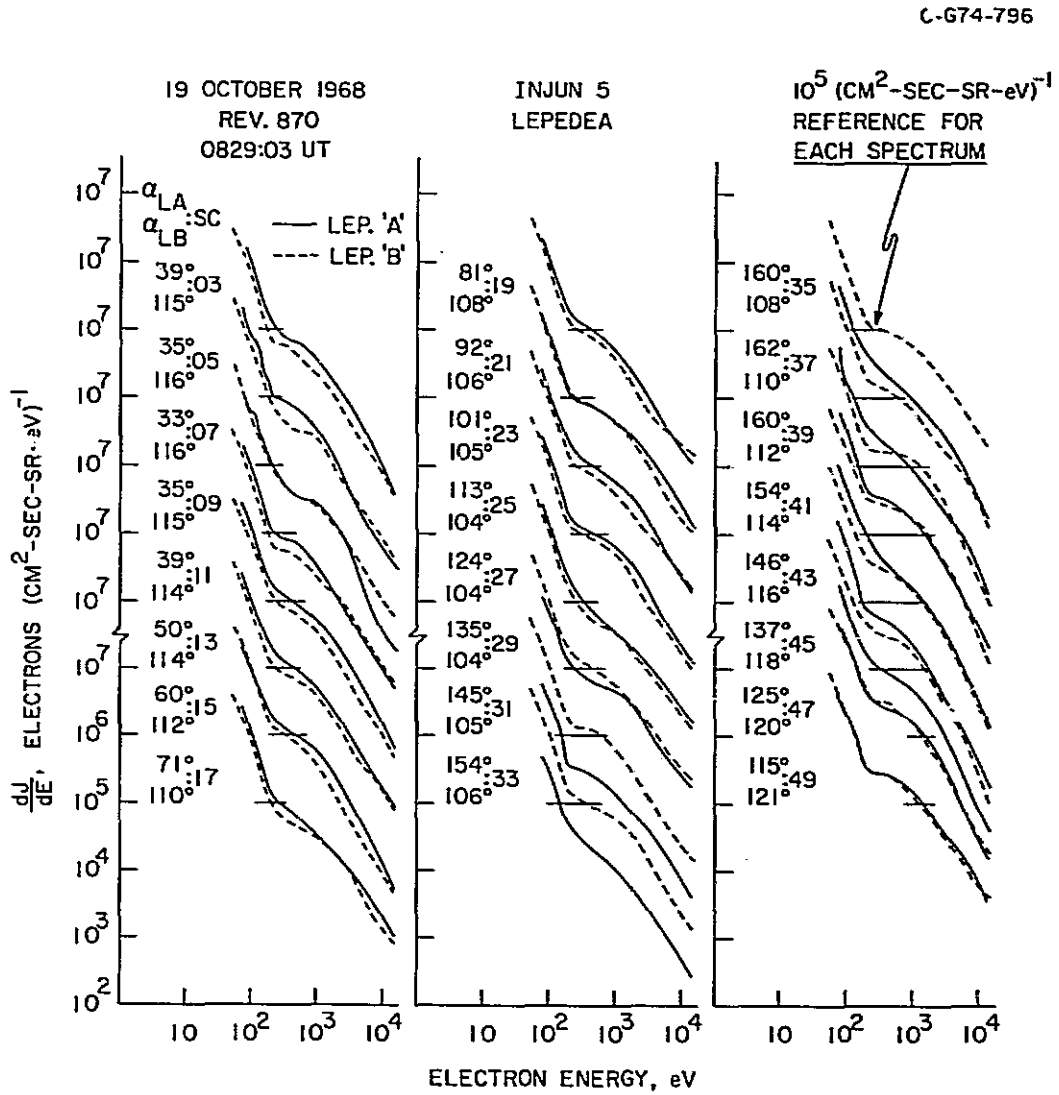
C-G74-796
19 OCTOBER 1968
REV. 870
0829:03 UT
INJUN 5
LEPEDEA
10^5 (CM^2-SEC-SR-eV)$^{-1}$
REFERENCE FOR
EACH SPECTRUM
α_{LA}:SC
α_{LB}:SC
LEP. 'A'
LEP. 'B'
39°:03
115°
35°:05
116°
33°:07
116°
35°:09
115°
39°:11
114°
50°:13
114°
60°:15
112°
71°:17
110°
81°:19
108°
92°:21
106°
101°:23
105°
113°:25
104°
124°:27
104°
135°:29
104°
145°:31
105°
154°:33
106°
160°:35
108°
162°:37
110°
160°:39
112°
154°:41
114°
146°:43
116°
137°:45
118°
125°:47
120°
115°:49
121°
$\frac{dJ}{dE}$, ELECTRONS (CM^2-SEC-SR-eV)$^{-1}$
ELECTRON ENERGY, eV

Figure 3.

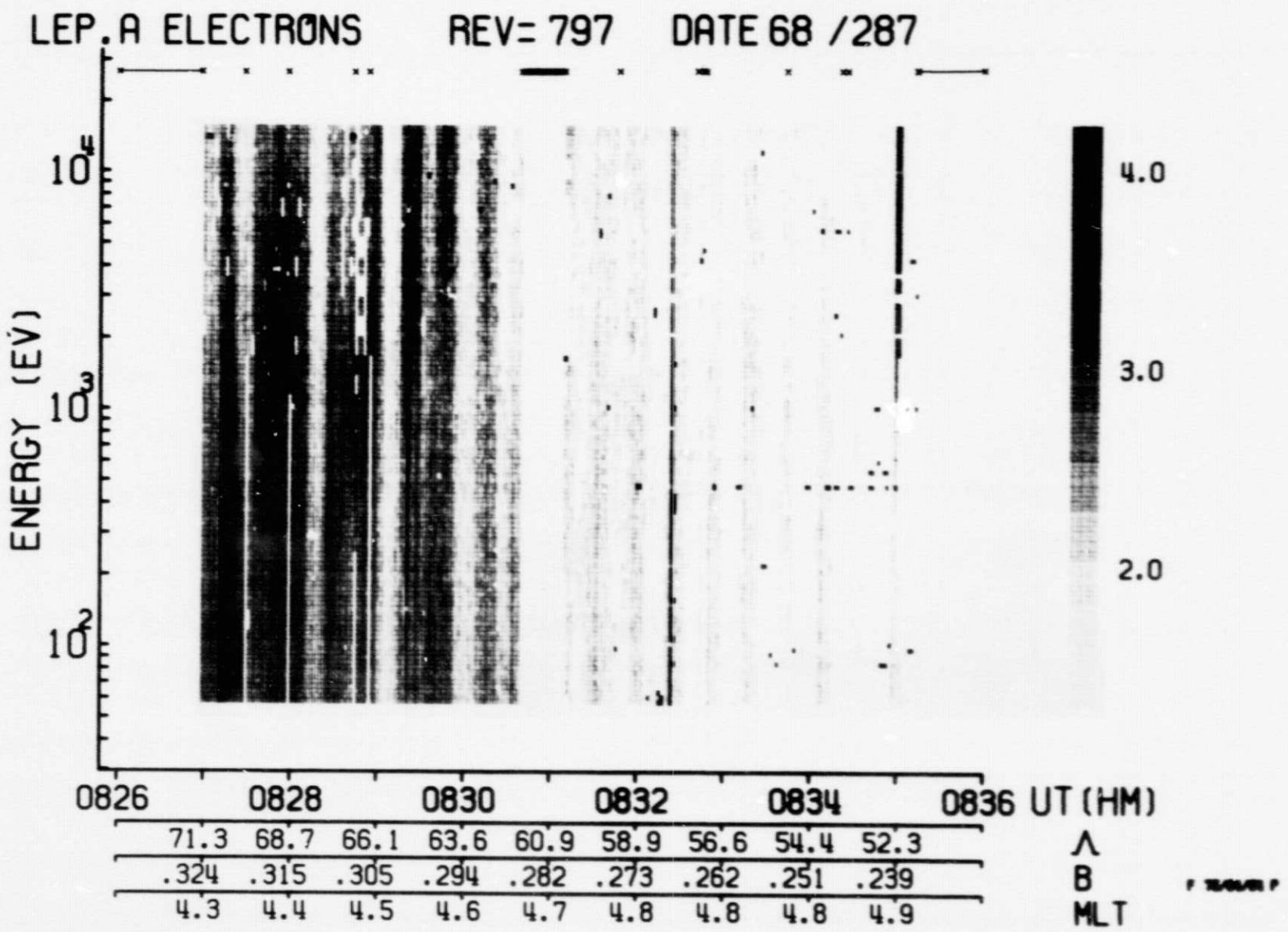

Figure 4.

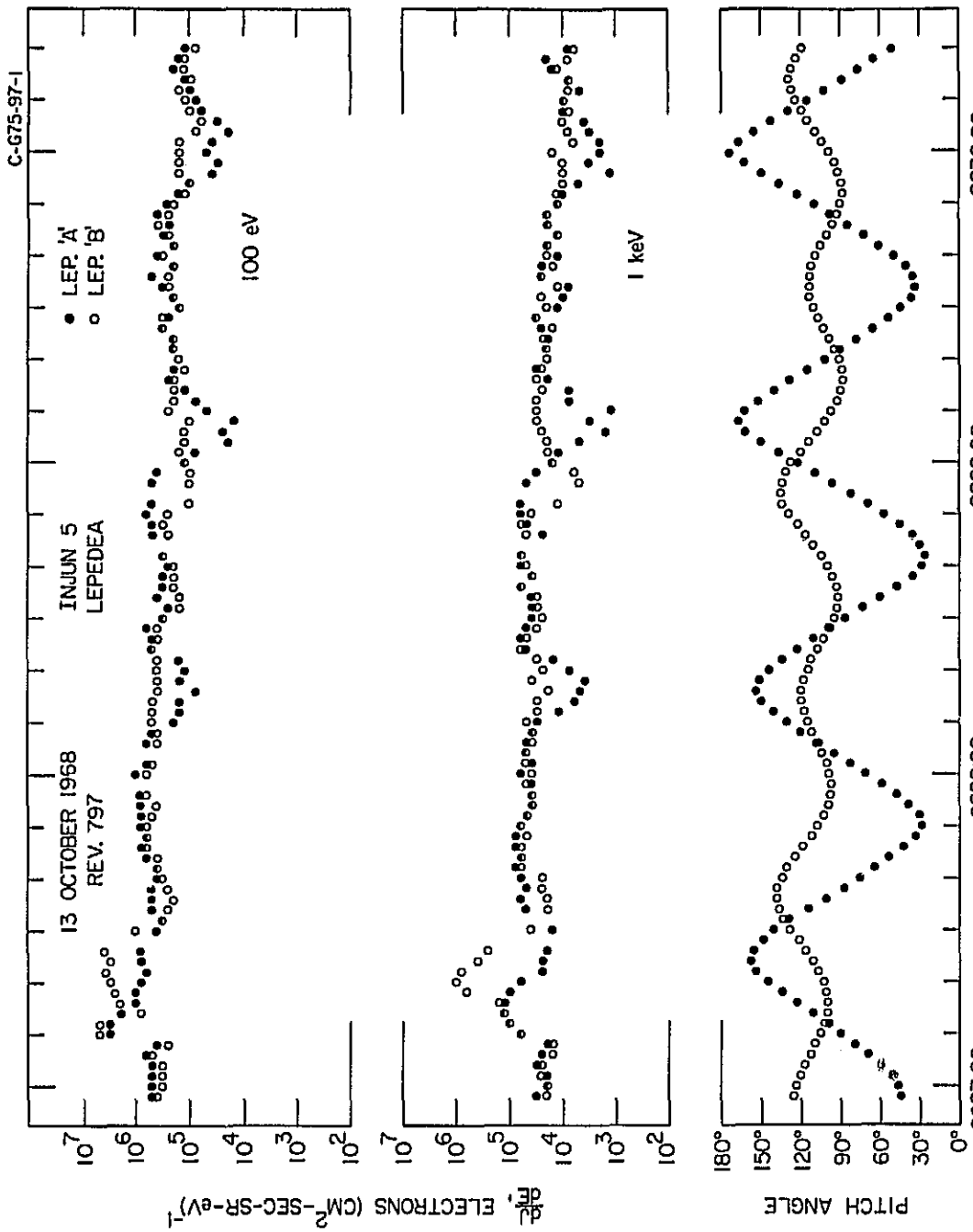
C-G75-97-1
13 OCTOBER 1968
REV. 797
INJUN 5
LEPEDEA
LEP. 'A'
LEP. 'B'
100 eV
1 keV
ELECTRONS (CM²-SEC-SR-eV)⁻¹
PITCH ANGLE
180°
150°
120°
90°
60°
30°
0°
0827:00
0828:00
0829:00
0830:00
U.T.

Figure 5.

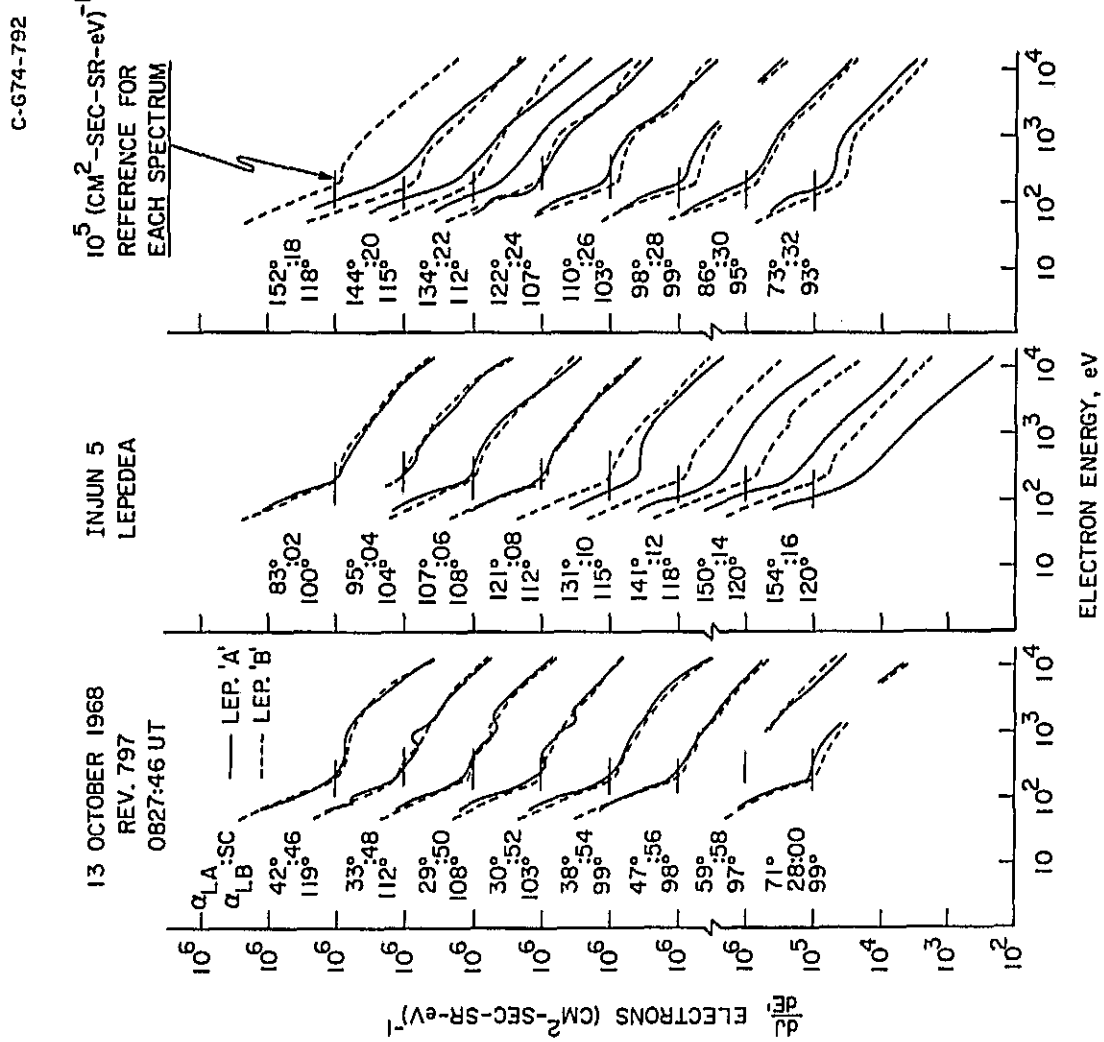
C-674-792
13 OCTOBER 1968
REV. 797
0827:46 UT
INJUN 5
LEPEDEA
10^5 (CM^2-SEC-SR-eV)$^{-1}$
REFERENCE FOR
EACH SPECTRUM
α_{LA}:SC
α_{LB}
LEP. 'A'
LEP. 'B'
ELECTRONS (CM^2-SEC-SR-eV)$^{-1}$
ELECTRON ENERGY, eV

Figure 6.

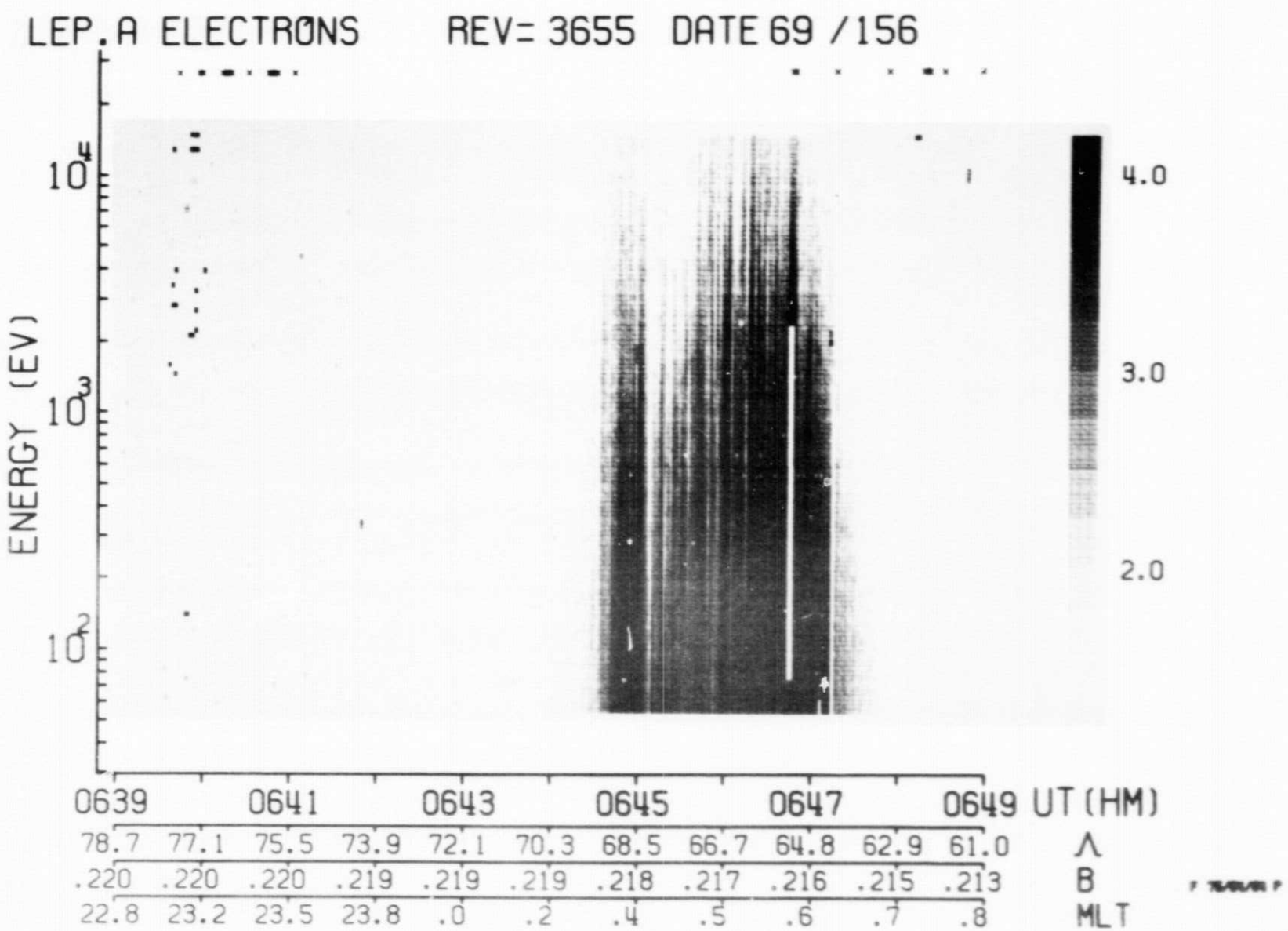

Figure 7.

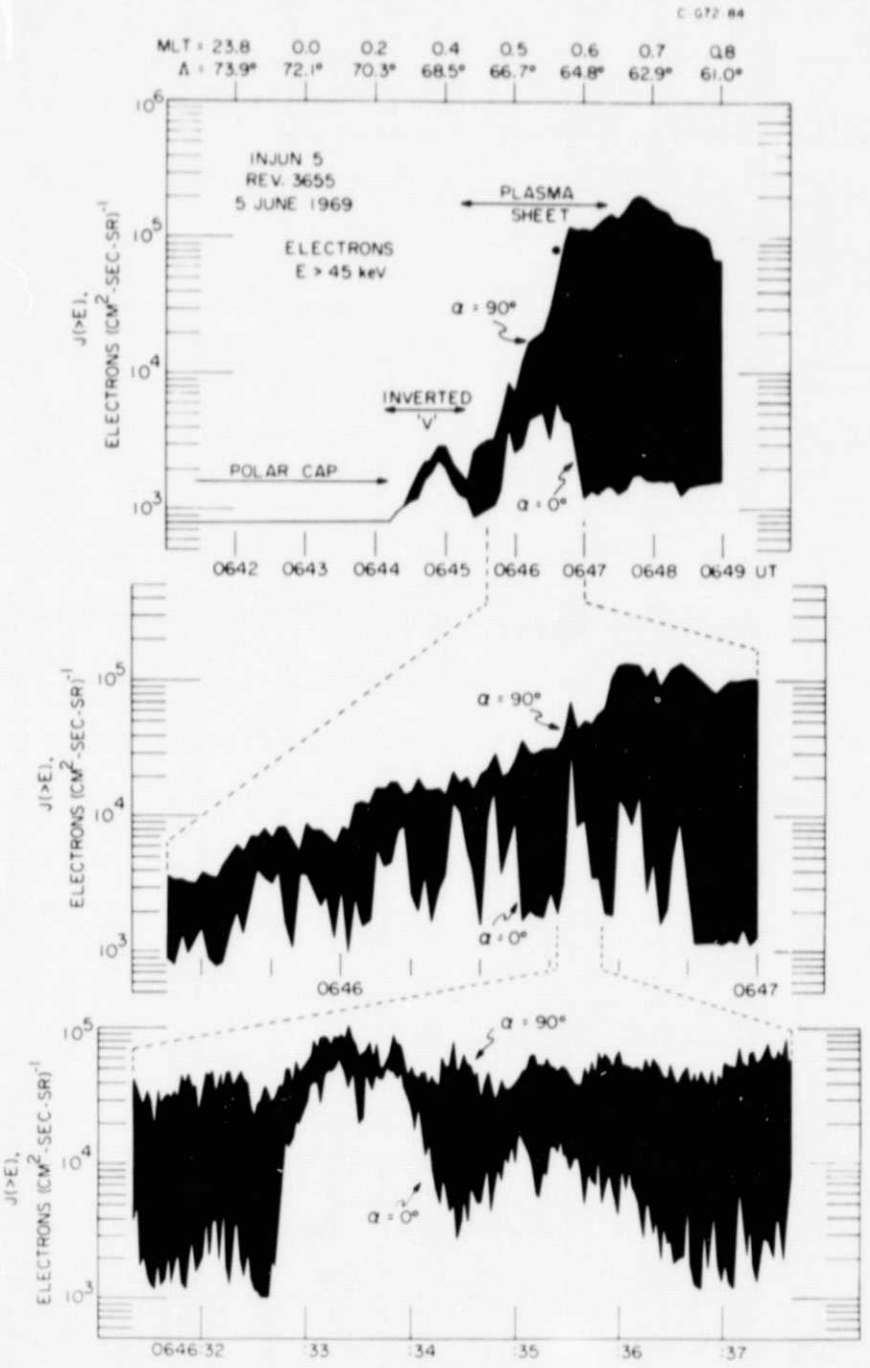
C-672-84
MLT = 23.8 0.0 0.2 0.4 0.5 0.6 0.7 0.8
Λ = 73.9° 72.1° 70.3° 68.5° 66.7° 64.8° 62.9° 61.0°
INJUN 5
REV. 3655
5 JUNE 1969
ELECTRONS
E > 45 keV
PLASMA SHEET
α = 90°
INVERTED 'V'
POLAR CAP
α = 0°
J(>E), ELECTRONS (CM²-SEC-SR)⁻¹
0642 0643 0644 0645 0646 0647 0648 0649 UT
0646
0647
0646:32 :33 :34 :35 :36 :37

Figure 8.

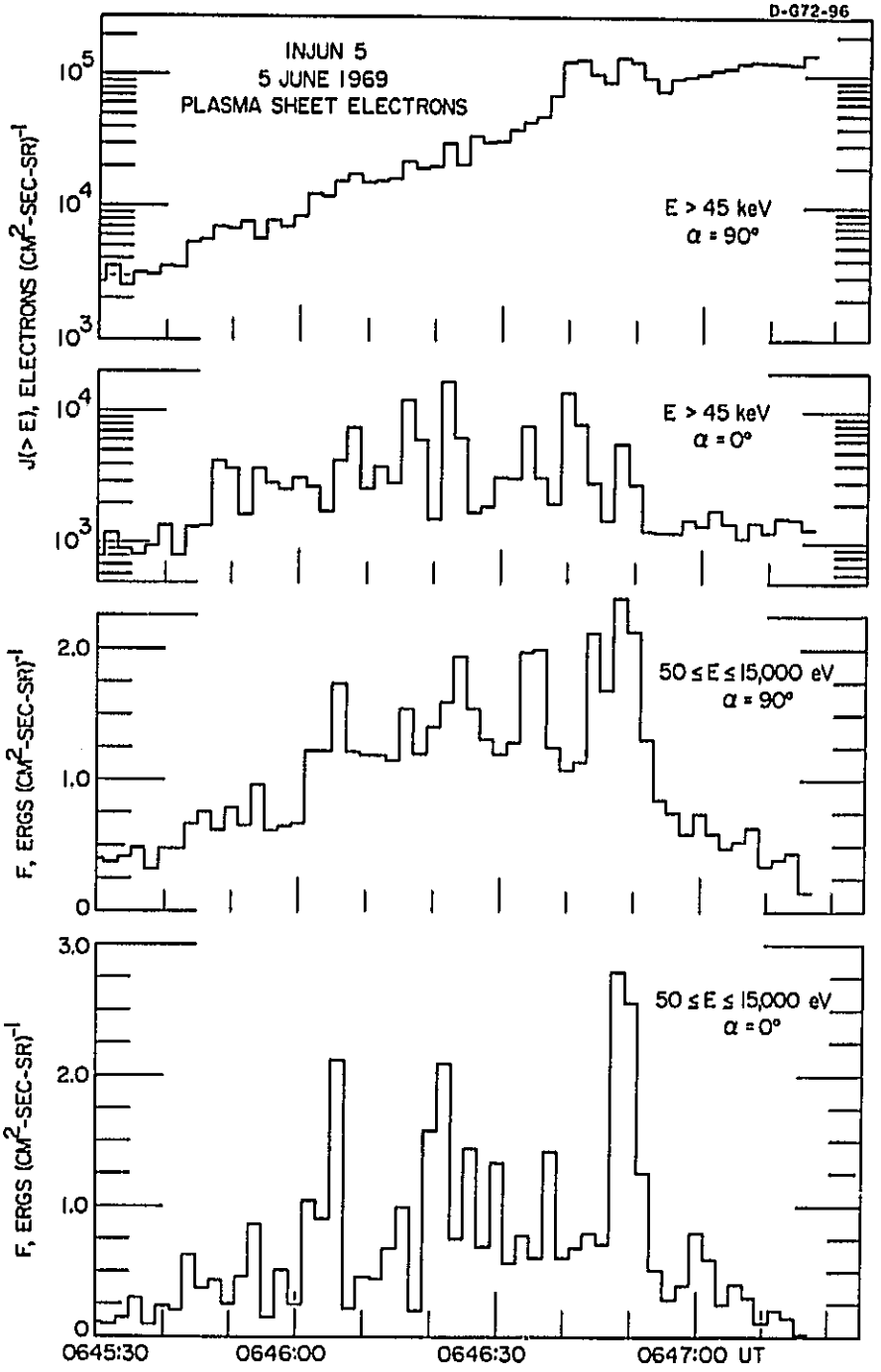

Figure 9.

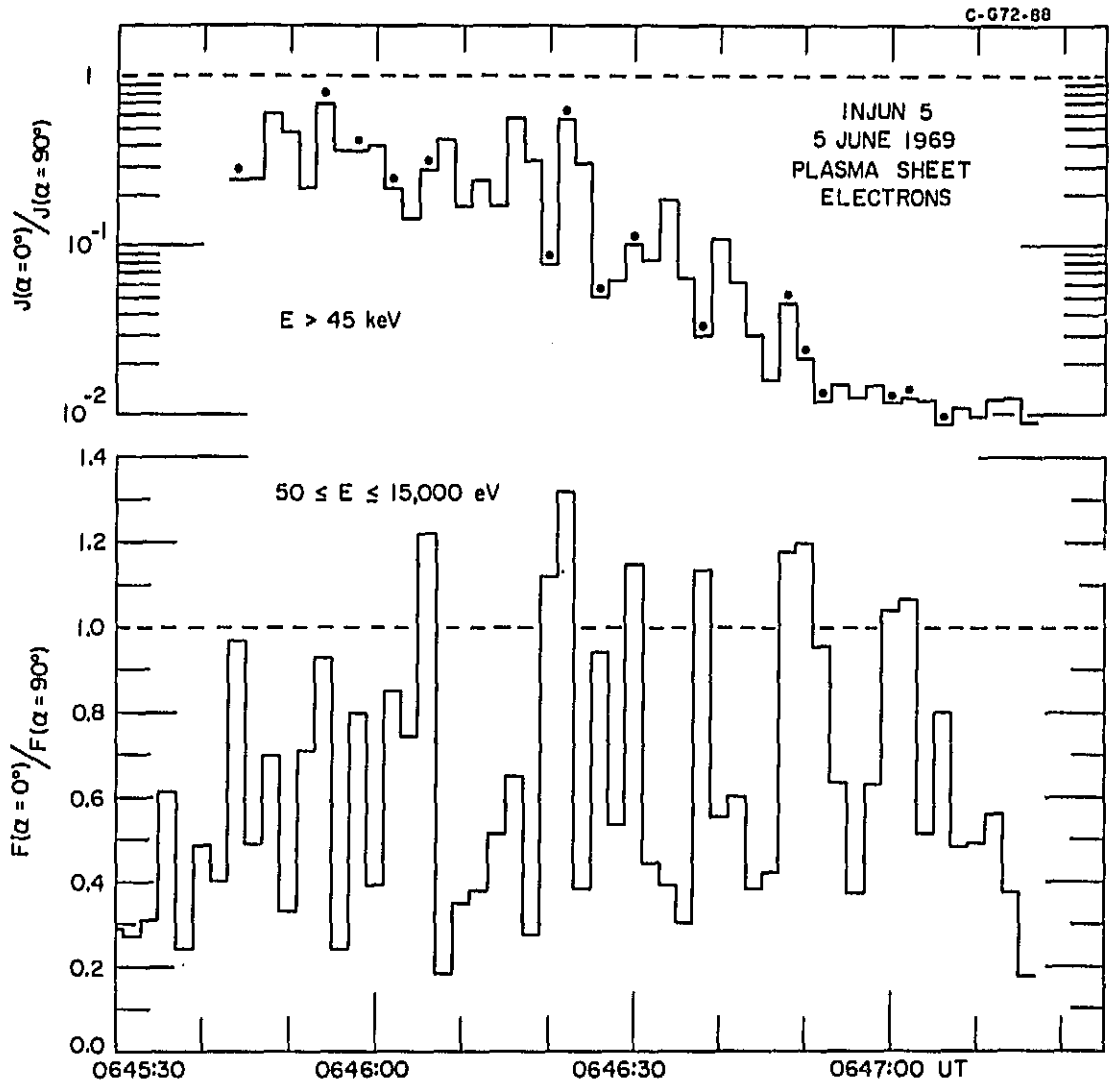
C-G72-68
INJUN 5
5 JUNE 1969
PLASMA SHEET
ELECTRONS
E > 45 keV
J(α=0°)/J(α=90°)
1
10⁻¹
10⁻²
50 ≤ E ≤ 15,000 eV
F(α=0°)/F(α=90°)
1.4
1.2
1.0
0.8
0.6
0.4
0.2
0.0
0645:30
0646:00
0646:30
0647:00 UT

Figure 10.

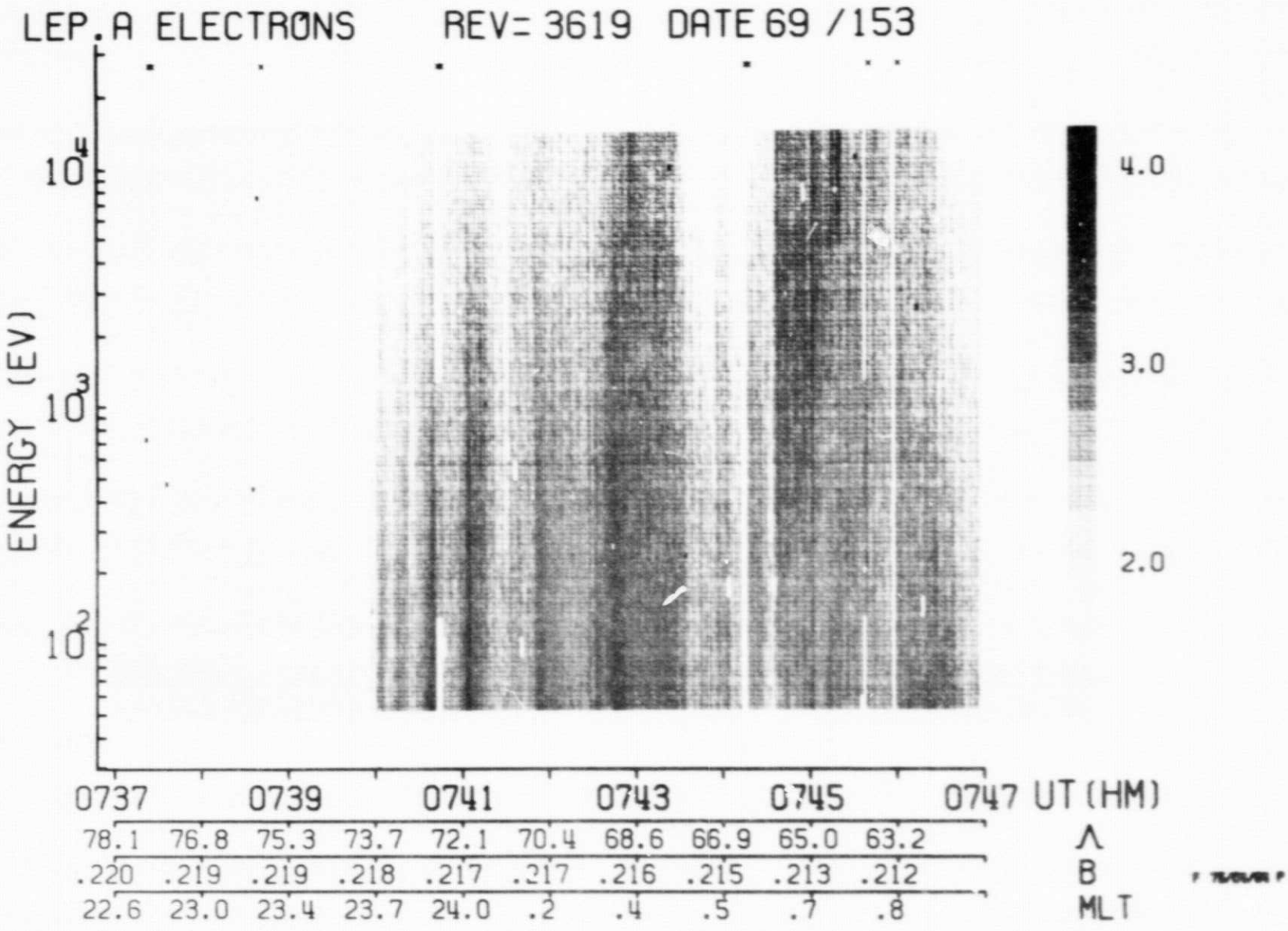

Figure 11.

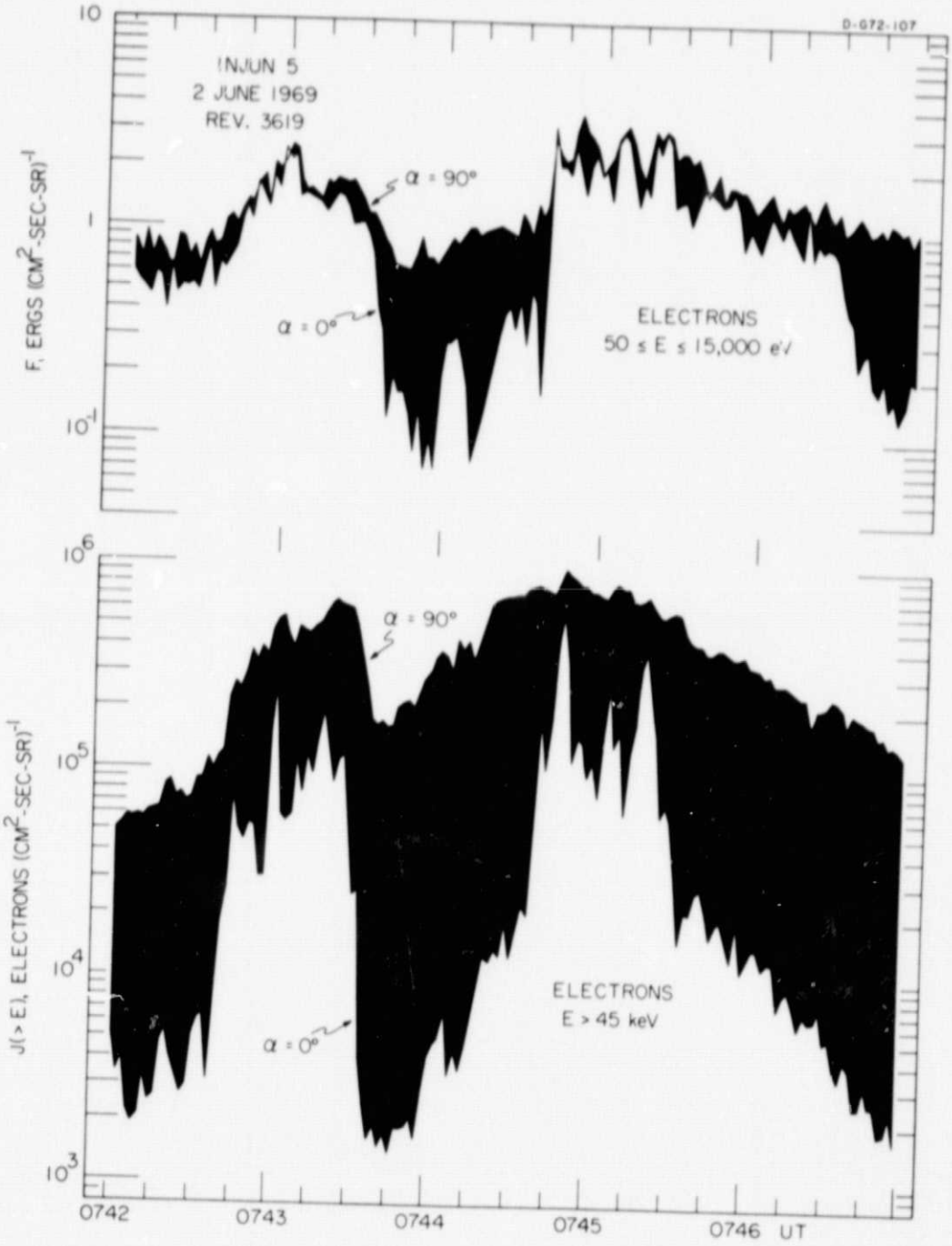
D-672-107
INJUN 5
2 JUNE 1969
REV. 3619
α = 90°
α = 0°
ELECTRONS
50 ≤ E ≤ 15,000 eV
F, ERGS (CM²-SEC-SR)⁻¹
10
1
10⁻¹
α = 90°
α = 0°
ELECTRONS
E > 45 keV
J(> E), ELECTRONS (CM²-SEC-SR)⁻¹
10⁶
10⁵
10⁴
10³
0742
0743
0744
0745
0746 UT

Figure 12.

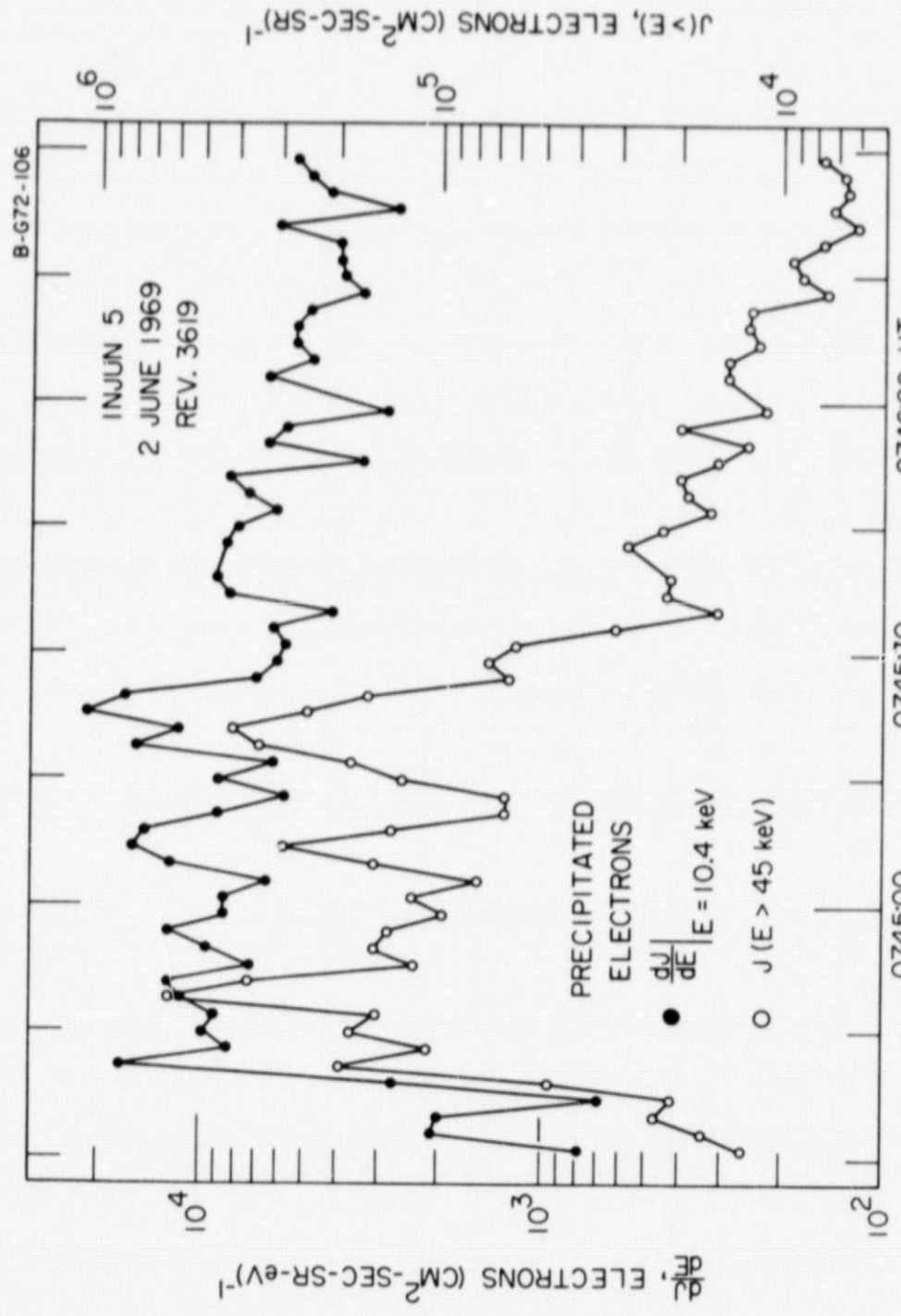

Figure 13.